

Supporting Information

Astatine partitioning between nitric acid and conventional solvents: Indication of covalency in ketone complexation of AtO⁺

Jonathan D. Burns^{*1}, Evgeny E. Tereshatov², Mallory A. McCarthy^{2,3}, Lauren A. McIntosh², Gabriel C. Tabacaru², Xin Yang³, Michael B. Hall³, and Sherry J. Yennello^{2,3}

¹Nuclear Engineering and Science Center, Texas A&M University, College Station, TX 77843, USA

²Cyclotron Institute, Texas A&M University, College Station, TX 77843, USA

³Department of Chemistry, Texas A&M University, College Station, TX 77843, USA

*e-mail: burns.jon@tamu.edu

Materials:

Nitric Acid (67–70% Aristar® Plus, HNO₃) was purchased from BDH chemicals; diisopropyl ether (ACS Grade ≥99%), 3-octanone (ACS Grade ≥96%), and 1-decanol (ACS Grade ≥99%) were purchased from EMD Millipore Corp.; 1-octanol (Lab grade) was purchased from Ward's Science; and methyl isobutyl ketone (ACS Grade ≥ 98.5%) was purchased from J. T. Baker, and all were used as received. Deionized (DI) H₂O was obtained from an ELGA LabWater Purelab Flex ultrapure laboratory water purification system operated at 18.2 MΩ cm at 25 °C.

Bismuth-207 was purchased from Eckert & Ziegler Isotope Products (Valencia, Ca) as a Bi(NO₃)₃ solution with ~8.9 kBq per mL and roughly 48 μM total Bi concentration in 4 M HNO₃. Astatine-211 was produced by the ²⁰⁹Bi(α,2n)²¹¹At nuclear reaction via α-particle bombardment of natural Bi metal target (isotopically pure ²⁰⁹Bi, metal purity ≥99.997% purchased from Goodfellow) for approximately 8 h with a beam current of 4–8 μA on the K150 cyclotron at Texas A&M. The α-particle beam energy was adjusted to 28.8 MeV prior to placing the beam on the target and was maintained for the duration of the bombardment. The Bi metal target (see Fig. S1) was about 9.4 g in mass with a geometry of a semi-rectangular shape (2.75×0.5 in), capped with half circles (radii 0.25 in) on either end with an estimated thickness of 950 μm and was housed in an aluminum frame (6061 Al alloy, 95% Al) in contact with a support block cooled by recirculated deionized water. The target was held at a 10° angle from to the beam to allow almost complete coverage of the target, while minimizing the loss of beam to the Al housing. **WARNING:** ²¹¹At, and to a lesser extent ²⁰⁷Bi, are all highly radioactive and were handled under ALARA principles in laboratories equipped to handle radioactive materials appropriately, a radiological biosafety cabinet was employed.

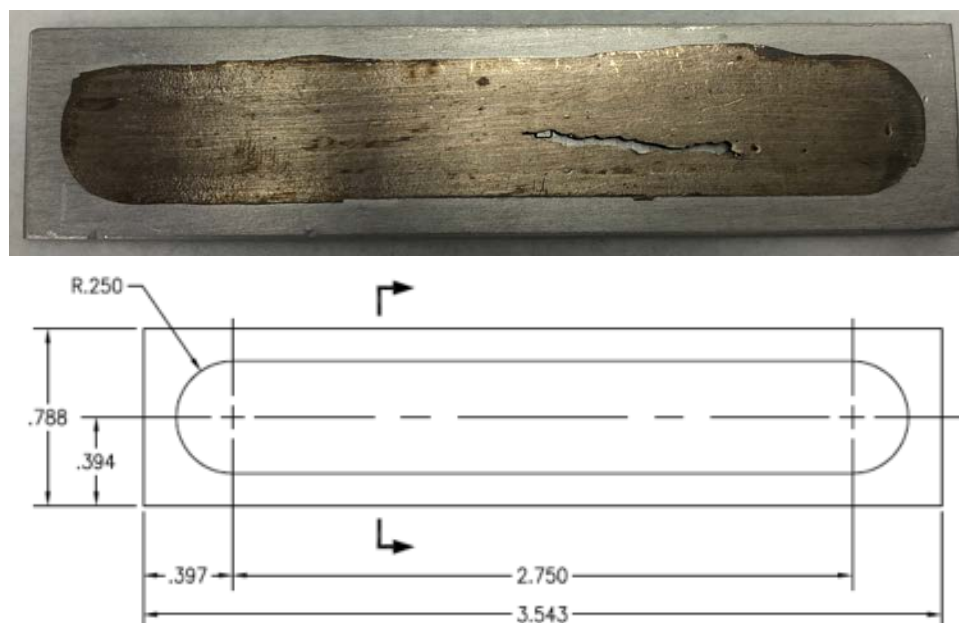


Fig. S1 Bismuth target on aluminum frame (top) and drawing of aluminum frame (bottom).

Table S1. Polarity for the selected organic solvents

Solvent	Dielectric Constant ¹
methyl isobutyl ketone	13.11
3-octanone	10.50
1-octanol	10.30
1-decanol	7.93
diisopropyl ether	3.81

Experimental:

Approximately one third of the bombarded target was dissolved by placing it on-end in a 50-mL centrifuge tube (see Fig. S2), to which 5 mL of H₂O and 10 mL of 15.8 M HNO₃ was added. The addition of HNO₃ produced a vigorous reaction with the Bi metal, resulting in the evolution of dark brown/red gas, presumable NO_x. To ensure no bubbles reached the top of the of the centrifuge tube, spreading contamination in the workspace, no attempt was made to add more HNO₃ and dissolve the entire target. The resulting solution was sampled in triplicate of 100- μ L aliquots and was found to contain 290 ± 30 MBq, with the overall activity of the target equaling 890 ± 80 MBq. Quantitative analysis was performed via gamma (γ)-ray spectroscopy using a calibrated Canberra Model GC4018 high-purity germanium detector (HPGe) with an active detector volume of ~ 45 cm³ and LynxTM digital signal analyzer (DSA, Canberra Industries Inc., Meriden, CT) along with Genie-2000 software. The detector has an energy resolution of 0.925 keV at 122 keV and 1.8 keV at 1300 keV. Relevant nuclear data were obtained from Browne and Firestone.³⁹ All calibrations were determined with a ¹⁵²Eu standard γ -ray source traceable to the National Institute of Standards and Technology (NIST) purchased from Eckert & Ziegler Isotope Products. The ²⁰⁷Bi was tracked directly by using the 1064 keV γ -ray. The ²¹¹At was tracked both directly by using the 79.9 keV, 89.8 keV, and 92.3 keV X-rays and 687 keV γ -ray and indirectly by using the ²¹¹Po 898 keV γ -ray.

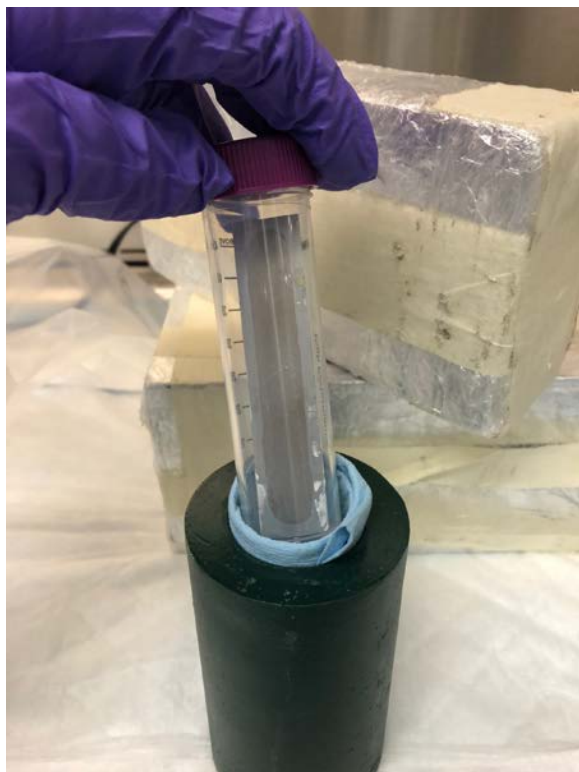


Fig. S2 Bombarded target on-end in 50-mL centrifuge tube.

Small batch liquid-liquid extraction experiments were conducted by interacting 500 μL of aqueous phase containing both the Bi and At with 500 μL of organic phase of either OctOH, 1-decanol, 3-octanone, methyl isobutyl ketone, or diisopropyl ether, so that the volume phase ratio was 1:1. The two phases were mixed by vigorous shaking for several seconds followed by end-over-end tumbling on a VWR® Tube Rotator at roughly 18 rpm for a minimum of 10 min. The samples were then centrifuged on a SCILOGEX D1008 Mini Centrifuge at 7,000 rpm for at least 5 min. 200 μL aliquots for both the aqueous and organic phases were samples for analysis by γ -ray spectroscopy. All experiments were performed in triplicates. In addition to the HPGe, a PerkinElmer 2480 WIZARD²® Automatic Gamma Counters with a well-type NaI detector and a HIDEX AMG Automatic Gamma counter with a well-type NaI detector were employed to assay samples.

D-values were calculated by taking the ratio of the activity of a particular species in the organic phase over that in the aqueous phase as shown in Eq. (1)

$$D = \frac{A_{org}}{A_{aq}} \cdot \frac{V_{aq}}{V_{org}} \quad (1)$$

where, A_{org} and A_{aq} are activities in organic and aqueous phases, respectively, and V is the volume of the particular phase.

DFT Calculations:

DFT calculations were carried out in the gas phase using Gaussian 16¹, Revision B.01. The B3LYP^{2,3} functional was selected to determine structural and energetic properties. A combination of small-core fully relativistic pseudopotential ECP60MDF⁴ with the corresponding AVTZ-PP basis set for At and 6-311G*^{5,6} for C, H, and O atoms was employed for geometry optimization in singlet state. Frequency calculations were followed at the same level to ensure all structures were stationary points at local minima with zero imaginary frequency. The NBO 6.0⁷ was employed for natural bond orbital analysis. Binding energies were calculated from optimized AtO⁺_base complexes with relaxed AtO⁺ and base molecules. Single point calculations were performed at the same level of theory on gas-phase optimized geometries with CPCM implicit solvation model to obtain the solvent corrected binding free energies ΔG_{cpcm} . The Gaussian 16 built-in 2-octanone solvent was selected due to its similarity in dielectric constant with the experimentally used 3-octanone. Cartesian coordinates of optimized geometries are attached below.

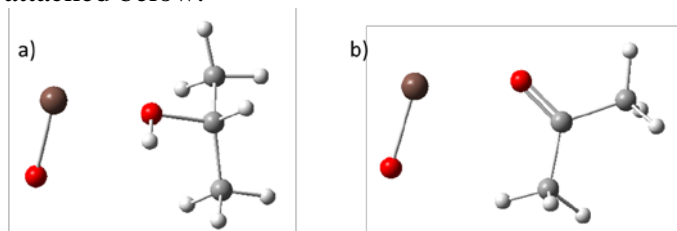


Fig. S3 Optimized geometry of a) AtO⁺_isopropanol b) AtO⁺_acetone.

Table S2. Selected geometric features from optimized geometries.

	d(At-O(intra))Å	d(At-O(inter))Å	O-At-O angle°	At-O=C angle°
AtO ⁺	1.914			
AtO ⁺ _isopropanol	1.913	2.317	105.5	
AtO ⁺ _acetone	1.916	2.326	107.0	132.2

Table S3. Binding energies of AtO⁺_isopropanol and AtO⁺_acetone complexes. (*Ee*, electronic energy; *H*, enthalpy; *G*, Gibbs free energy; *G*_{cpcm}, solvent corrected Gibbs free energy).

	AtO ⁺ _isopropanol	AtO ⁺ _acetone
ΔE_e (kcal/mol)	-52.4	-56.0
ΔH (kcal/mol)	-51.5	-54.5
ΔG (kcal/mol)	-42.6	-47.2
ΔG_{cpcm} (kcal/mol)	-29.8	-31.9

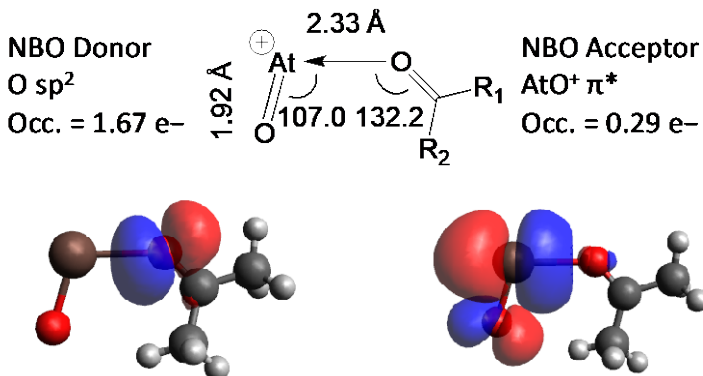


Fig. S4 NBO analysis of AtO⁺_acetone complex.

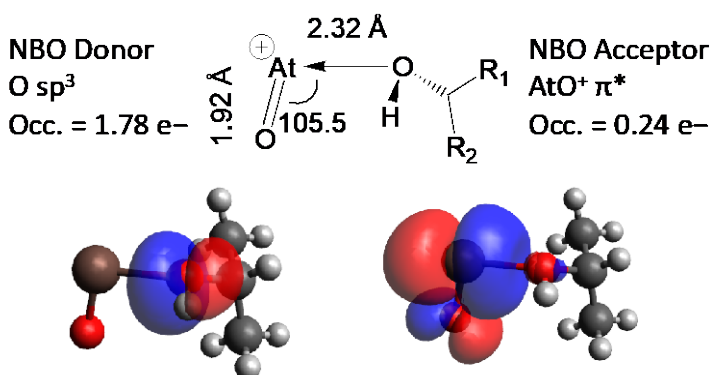


Fig. S5 NBO analysis of AtO⁺_isopropanol complex.

References

- (1) W. M. Haynes, Ed., *CRC Handbook of Chemistry and Physics*, CRC Press, Boca Raton, FL, 97th edn., 2016.
- (2) Gaussian 16, Revision B.01, Frisch, M. J. *et al.* Gaussian, Inc., Wallingford CT, 2016
- (3) Becke, A. D. Density-Functional Exchange-Energy Approximation with Correct Asymptotic Behavior. *Phys. Rev. A* **1988**, 38 (6), 3098–3100. <https://doi.org/10.1103/PhysRevA.38.3098>.
- (4) Becke, A. D. Density-functional Thermochemistry. III. The Role of Exact Exchange. *J. Chem. Phys.* **1993**, 98 (7), 5648–5652. <https://doi.org/10.1063/1.464913>.
- (5) Peterson, K. A.; Figgen, D.; Goll, E.; Stoll, H.; Dolg, M. Systematically Convergent Basis Sets with Relativistic Pseudopotentials. II. Small-Core Pseudopotentials and Correlation Consistent Basis Sets for the Post-*d* Group 16–18 Elements. *J. Chem. Phys.* **2003**, 119 (21), 11113–11123. <https://doi.org/10.1063/1.1622924>.
- (6) Krishnan, R.; Binkley, J. S.; Seeger, R.; Pople, J. A. Self-consistent Molecular Orbital Methods. XX. A Basis Set for Correlated Wave Functions. *J. Chem. Phys.* **1980**, 72 (1), 650–654. <https://doi.org/10.1063/1.438955>.
- (7) Frisch, M. J.; Pople, J. A.; Binkley, J. S. Self-consistent Molecular Orbital Methods 25. Supplementary Functions for Gaussian Basis Sets. *J. Chem. Phys.* **1984**, 80 (7), 3265–3269. <https://doi.org/10.1063/1.447079>.
- (8) *NBO 6.0* Glendening, E.D. *et al.* Theoretical Chemistry Institute, University of Wisconsin, Madison (2013).

- (9) Douglas, M.; Kroll, N. M. Quantum Electrodynamical Corrections to the Fine Structure of Helium. *Ann. Phys.* **1974**, *82* (1), 89–155. [https://doi.org/10.1016/0003-4916\(74\)90333-9](https://doi.org/10.1016/0003-4916(74)90333-9).
- (10) Hess, B. A. Applicability of the No-Pair Equation with Free-Particle Projection Operators to Atomic and Molecular Structure Calculations. *Phys. Rev. A* **1985**, *32* (2), 756–763. <https://doi.org/10.1103/PhysRevA.32.756>.
- (11) Visscher, L.; Dyall, K. G. DIRAC–FOCK ATOMIC ELECTRONIC STRUCTURE CALCULATIONS USING DIFFERENT NUCLEAR CHARGE DISTRIBUTIONS. *At. Data Nucl. Data Tables* **1997**, *67* (2), 207–224. <https://doi.org/10.1006/adnd.1997.0751>.
- (12) Bross, D. H.; Peterson, K. A. Correlation Consistent, Douglas–Kroll–Hess Relativistic Basis Sets for the 5p and 6p Elements. *Theor. Chem. Acc.* **2014**, *133* (2). <https://doi.org/10.1007/s00214-013-1434-9>.
- (13) Dunning, T. H. Gaussian Basis Sets for Use in Correlated Molecular Calculations. I. The Atoms Boron through Neon and Hydrogen. *J. Chem. Phys.* **1989**, *90* (2), 1007–1023. <https://doi.org/10.1063/1.456153>.

Cartesian Coordinates

AtO⁺

At	0.000000	0.000000	0.164639
O	0.000000	0.000000	-1.749286

AtO⁺_isopropanol

At	-0.854424	-0.132260	-0.023366
O	-0.968508	1.665960	0.619481
C	2.617671	-0.226701	-0.264731
O	1.252114	-0.320136	-0.969860
C	3.012377	1.226195	-0.123973
H	2.349823	1.765400	0.556255
H	3.034116	1.744104	-1.086378
H	4.024752	1.277151	0.285324
C	2.513460	-1.010894	1.018624
H	1.889071	-0.508320	1.762603
H	3.512653	-1.098761	1.452287
H	2.145446	-2.024196	0.847512
H	1.290795	0.142268	-1.823005
H	3.249463	-0.753718	-0.984992

AtO⁺_acetone

At	0.869110	-0.179961	0.025053
O	1.014505	1.700834	-0.308553
C	-2.426900	-0.004799	-0.001867
O	-1.394262	-0.712116	-0.052305
C	-2.409082	1.468330	0.211228
H	-1.512939	1.951454	-0.175453

H	-2.435548	1.639223	1.297172
H	-3.302007	1.936337	-0.202826
C	-3.728269	-0.718357	-0.139953
H	-4.159330	-0.450521	-1.113287
H	-4.431132	-0.362368	0.619324
H	-3.609852	-1.798210	-0.084016

Isopropanol

C	0.00231000	0.03844600	0.36460500
O	-0.02909500	1.36790400	-0.16651300
C	-1.20926000	-0.76662000	-0.10302100
H	-1.23103100	-0.81881300	-1.19503700
H	-2.14372500	-0.30206100	0.23069000
H	-1.19114300	-1.78618600	0.29377000
C	1.32179500	-0.56633600	-0.08817700
H	1.35887800	-0.61999500	-1.17973700
H	1.45222400	-1.57424600	0.31447400
H	2.15629700	0.05242200	0.24816900
H	-0.85093300	1.78605800	0.11430900
H	-0.00687500	0.08665100	1.46503300

Acetone

C	0.00000000	0.00000000	0.18716000
O	0.00000000	0.00000000	1.39614200
C	0.00000000	-1.29140400	-0.61333600
H	0.00000000	-2.14490300	0.06333100
H	0.87851100	-1.34351200	-1.26468000
H	-0.87851100	-1.34351200	-1.26468000
C	0.00000000	1.29140400	-0.61333600
H	-0.87851100	1.34351200	-1.26468000
H	0.87851100	1.34351200	-1.26468000
H	0.00000000	2.14490300	0.06333100